Cascade-Type Prelithiation Approach for Li-Ion Capacitors

Bihag Anothumakkool, Simon Wiemers-meyer, Dominique Guyomard, Martin Winter, Thierry Brousse, Joël Gaubicher

ADVANCED ENERGY MATERIALS

Postfach 10 11 61
69451 Weinheim
Germany
Courier services:
Boschstraße 12
69469 Weinheim
Germany
Tel.: (+49) 6201 606 531
Fax: (+49) 6201 606 500
E-mail: advenergymat@wiley.com

WILEY-VCH

Dear Author,

Please correct your galley proofs carefully and return them no more than four days after the page proofs have been received.

Please limit corrections to errors already in the text; cost incurred for any further changes or additions will be charged to the author, unless such changes have been agreed upon by the editor.

The editors reserve the right to publish your article without your corrections if the proofs do not arrive in time.

Note that the author is liable for damages arising from incorrect statements, including misprints.

Please note any queries that require your attention. These are indicated with a Q in the PDF and a question at the end of the document.

Reprints may be ordered by filling out the accompanying form.

Return the reprint order form by fax or by e-mail with the corrected proofs, to Wiley-VCH : advenergymat@wiley.com

To avoid commonly occurring errors, **please ensure that the following important items are correct** in your proofs (please note that once your article is published online, no further corrections can be made):

- **Names** of all authors present and spelled correctly
- **Titles** of authors correct (Prof. or Dr. only: please note, Prof. Dr. is not used in the journals)
- **Addresses** and **postcodes** correct
- **E-mail address** of corresponding author correct (current email address)
- **Funding bodies** included and grant numbers accurate
- **Title** of article OK
- All **figures** included
- **Equations** correct (symbols and sub/superscripts)

Corrections should be made directly in the PDF file using the PDF annotation tools. If you have questions about this, please contact the editorial office. The corrected PDF and any accompanying files should be uploaded to the journal's Editorial Manager site.

Author Query Form

WILEY

Journal AENM

Article aenm201900078

Dear Author,

During the copyediting of your manuscript the following queries arose.

Please refer to the query reference callout numbers in the page proofs and respond to each by marking the necessary comments using the PDF annotation tools.

Please remember illegible or unclear comments and corrections may delay publication.

Many thanks for your assistance.

Query No.	Description	Remarks
Q1	Please provide TOC keyword & TOC Figure.	
Q2	Please spell out the full first name of D. Guyomard in the byline.	
Q3	Please confirm that forenames/given names (blue) and surnames/family names (vermilion) have been identified correctly.	
Q4	Please provide the highest academic title (either Dr. or Prof.) for all authors, where applicable.	
Q5	Please shorten Abstract text to a maximum of 200 words.	
Q6	Please provide Table of Contents text (maximum of 60 words). All abbreviations should be defined.	
Q7	Experimental section has been moved at the end of section as per journal style. Please check for correctness.	
Q8	Please check all equations have been correctly typeset.	

Q1 xxxx

FPO

XXXX Q6

ADVANCED ENERGY MATERIALS

www.advenergymat.de

Cascade-Type Prelithiation Approach for Li-Ion Capacitors

Bihag Anothumakkool, Simon Wiemers-Meyer, D. Guyomard, Martin Winter, Thierry Brousse,* and Joel Gaubicher*

This study reports on a novel method of prelithiation to balance the irreversible capacity occurring during the first charge of lithium-ion capacitors, which is the prime bottleneck to be addressed for their efficient integration in practical application. Based on a composite positive electrode that integrates pyrene monomers and an insoluble lithiated base, Li_3PO_4, a "cascade-type" process involving two consecutive irreversible reactions is proposed: i) oxidative electropolymerization of the pyrene moieties release electrons and protons; ii) protons are captured by Li_3PO_4 and exchanged by a stoichiometric amount of Li^+ into the electrolyte. (^1H, ^{19}F, and ^{31}P) NMR spectroscopy, operando XRD, as well as Raman spectroscopy data support this mechanism. By decoupling the irreversible source of lithium ions from electrons, the cascade-type prelithiation step allows, for the first time, to simultaneously enhance the capacity of the positive electrode, thanks to p-doping of the resulting polymer. Remarkably, the proton scavenging property of Li_3PO_4 also boosts the polymerization process, which enables a 16% increase in capacity without detrimental effect on power properties and cycle life. As a proof of concept, full cells integrating a cheap carbon black based negative electrode, show much-improved capacity of 17 mAh $g^{-1}_{electrodes}$ (44 F $g^{-1}_{electrodes}$, 3–4.4 V) and excellent stability over 2200 cycles at 1 A g^{-1}. Thanks to its versatile chemistry and flexibility this approach in principle can be applied to any kind of ion batteries.

1. Introduction

Clean and versatile energy storage technologies play a pivotal role in the successful integration of renewable energy sources into key economic sectors such as electromobility and grid storage.[1,2] In this regard and thanks to their high energy efficiency and scalability, the high energy lithium-ion batteries (LIB) and complimentary high power lithium-ion capacitors (LIC) have been successfully introduced as the technologies of choice.[3–8] However, the main Achilles' heel hindering intensive commercialization of these systems is rooted in the irreversible loss of charge (e^-) and active lithium (Li^+) during cycling, affecting Coulombic and energy efficiencies.[9] The main mechanism identified so far corresponds to the solid electrolyte interphase (SEI) formation at the negative electrode during the first charge.[10–12] Accordingly, a so-called prelithiation step that compensates for this Li^+ (and electron) loss is necessary to reach full utilization of the active materials. This is one of the major issues considered during the manufacture of LIB and LIC with high efficiency. Noteworthy, although they are common to both LIB and LIC, prelithiation is even more critical for LIC because any additional source of Li^+ ions should be large enough to not only address SEI formation but also to lithiate (on charge) the negative electrode. Accordingly, the accuracy of the prelithiation degree is lessened for LIC compared to that of LIB for which hazards associated with Li plating may arise. Prelithiation strategies and techniques have been extensively reviewed recently.[10] They can be classified into two main categories: The first one relies on a pretreatment step (chemical or electrochemical lithiation) of one of the electrode before cell assembly. In this case, main drawbacks are costs (mainly because of processing conditions require to handle the high sensitivity of reducing materials to ambient air), duration of this additional step as well as its integration within the production process. The use of a sacrificial Li metal foil directly or externally connected to graphite for prelithiation is one of the main approaches, most particularly for commercial LIC.[13–16] However, this method can lead to volume changes, short-circuiting, and thermal runaway[17] in addition to being time-consuming.[18] Other methods in this direction include electrochemical prelithiation of the negative electrode,[19–21] and stabilized lithium metal compounds (SLMP).[10,22] The interest in most of the methods

B. Anothumakkool, D. Guyomard, T. Brousse, J. Gaubicher
Institut des Materiaux Jean Rouxel (IMN)
University of Nantes
CNRS
2 rue de Houssiniere-B.P. 32229-44322,
Nantes cedex 3, France
E-mail: thierry.brousse@univ-nantes.fr; joel.gaubicher@cnrs-imn.fr
T. Brousse
Réseau sur le Stockage Electrochimique de l'Energie (RS2E)
FR CNRS
3459 France
B. Anothumakkool, S. Wiemers-Meyer, M. Winter
MEET Battery Research Center
Institute of Physical Chemistry
University of Münster
Corrensstr. 46, 48149 Münster, Germany
M. Winter
Helmholtz Institute Münster
IEK-12
Forschungszentrum Jülich GmbH
Corrensstraße 46, 48149 Münster, Germany
The ORCID identification number(s) for the author(s) of this article can be found under https://doi.org/10.1002/aenm.201900078.

DOI: 10.1002/aenm.201900078

cited above is, however, mitigated by the hazards and side reactions as well as complex processes associated with the manipulation of metallic lithium on an industrial scale.

The second prelithiation approach that is performed upon cell assembly during the formation cycles uses additives, either a lithiated sacrificial salt or an overlithiated material, integrated into the composite electrode. The capacity of these additives determines their ability to prelithiate the negative electrode.[9] However, unless their oxidized form is a gaz[23] and that can be removed by cell opening (sacrificial salts), or a competitive overlithiated Li storage material,[24] they constitute a dead mass (and volume) that mitigates the gain in energy density resulting from prelithiation. Many of these additives have also been shown to be poor conductors[23] and/or produce side reactions on cycling.[10,25] In addition, although this strategy in principle avoids a supplementary step, and therefore can be more easily integrated in a production process at lower costs, relevant materials were proved so far to be air-sensitive and/or react with polar solvents during the composite electrode processing.[10,23] Whereas most of these additives are inorganic materials, sacrificial organic Li salts have been proposed for the first time in 2008 by Armand and co-workers for LIB.[23] Several candidates such as azide, oxocarbons, dicarboxylates, and hydrazides were examined. Except for the oxalate these compounds were shown to release Li^+ below 4.2 V versus Li+/Li^0 while the anion converts to gaseous N_2, CO, or CO_2.[26] More recently, Jeżowski et al.[25] reported the use of the sacrificial and ecofriendly, 3,4-dihydroxybenzonitrile dilithium salt, as an additive of the positive electrode of LIC. The later releases Li ions during oxidation (at approximately 3 V) to the neutral dioxo form, which dissolves in the electrolyte. This approach is therefore twarthed not only with a "dead" mass (of low volumetric density) but also with an undeniable risk of redox shuttling. Furthermore, such as the majority of the (over)lithiated inorganic additives reported so far,[9] this organic additive is unstable in ambient air and endowed with a poor electron conductivity.

In conclusion although most of the above strategies are promising and successfully prelithiate the negative electrode of LIC or LIB recurrent issues strongly impede their manufacturing process: i) costs that are mainly due to handling conditions of ambient air-sensitive materials, time required for pretreatment steps and use of costly precursors; (ii) dead mass(volume) of prelithiation residue in the cell; (iii) poor electronic and/or ionic conductivity of additives (iv) possible unwanted chemical and/or redox side reactions with the electrolyte and/or solvents required for the electrode formulation. Today, prelithiation has only been commercialized for LIC by a single company (JMEnergy, Minato, Japan). Therefore, there exist unexplored solutions that can provide a good compromise for practical applications.

From our understanding, the main and common weakness of the previously cited approaches stems from the fact that the Li and electron sources are ascribed to a single lithiated compound (n-type). In that sense, the strategy proposed hereafter fundamentally departs from the state-of-the-art because electrons and lithium-ions arise from two consecutive reactions (cascade-type) putting at play two distinct additives integrated within the positive electrode; the first one being solely the electron source and the second, the Li^+ one. To reach this goal, the key feature of the prelithiation process is to pair an aromatic p-type redox material, the oxidation of which is counterbalanced by anion ingress and proton release within the desired potential range, and a lithium base that can exchange Li^+ for protons. In the following a pyrene monomer (1 \$ kg^{-1}) was selected i) during the first cycle, oxidative electropolymerization of pyrene produces oligomers and/or low order, small chain polymers with the simultaneous release of protons.[27–29] The resulting conjugated oligomers are condensed within the positive electrode and contribute to the overall capacity during subsequent cycles thanks to reversible p-doping.[30] The kinetics and capacity retention of this p-type system was proved to be outstanding particularly in the case of carbon-based positive electrodes.[31–33] ii) Second, a mass-produced lithiated base, Li_3PO_4 (p*K*a 12.2) captures the protons[31] and releases an equal number of Li^+ ensuring the prelithiation of the negative electrode (**Scheme 1**).

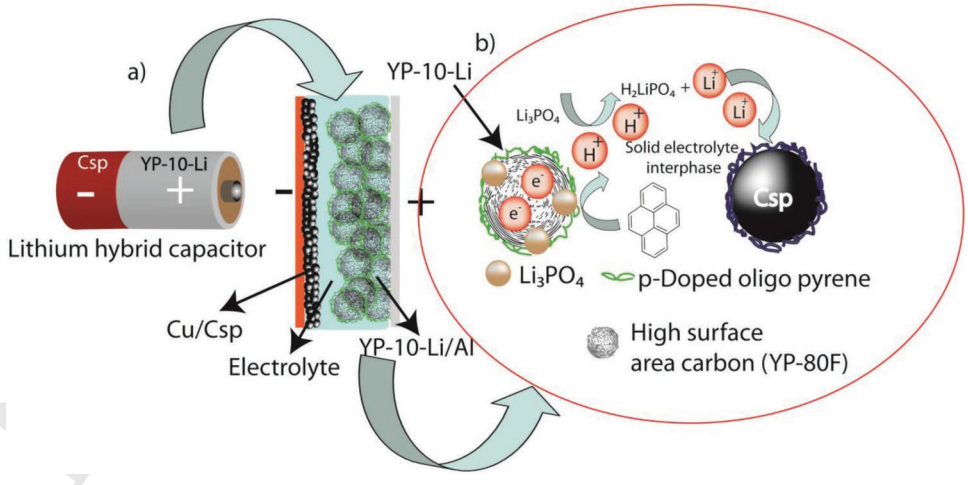

Scheme 1. Schematic representation of the new prelithiation strategy using a source of electrons from pyrene electropolymerization and, a source of lithium ions from a chemical reaction involving an insoluble inorganic base. a) Graphical representation of LIC and the individual components in the positive and negative electrodes in the cell, and b) pictorial representation of the prelithiation process occurring during the first charge via the cascade-type mechanism.

Significant advantages directly result from decoupling electron and Li^+ sources into two compounds: i) it offers much more flexibility and versatility because the chemistry and/or reactivity of one can in principle be adapted to a targeted application without impacting the other. For instance, the reactivity of the two compounds toward electrode formulation solvents, ambient air and electrolyte can be tailored separately which greatly facilitate industrial integration. Also, the Li^+ base can be easily changed for Na^+, K^+, Mg^{2+}, or Ca^{2+} ones to target various cell chemistry. ii) the redox potential of the monomer can be tuned between 4.5 and 3.5 V depending on the nature of the substituents which avoids electrolyte decomposition at high voltage[27,29] iii) the lithiated additive does not need to be an electron conductor.

In the following, we considered the LIC application for which prelithiation is more crucial. Our primary targets were first to prove and evaluate the efficiency of the cascade-type mechanism and to find an optimum electrode formulation. A proof of concept is then demonstrated in a full-cell using a cheap and abundant carbon black (Super P, Csp) as a negative electrode material.

2. Result and Discussion

A state-of-the-art supercapacitor carbon (YP-80F) was chosen for this study. YP-80F electrode is from now on referred to as YP-0, and the corresponding electrode composition is reported in **Table 1**. The specific surface area of YP-0 is ≈1000 $m^2\ g^{-1}$, which mostly stems from mesoporosity (Figure S1a, Supporting Information). The capacity of YP-0 was initially measured and found to be 40 mAh g^{-1} in a Li metal half-cell between 3 and 4.4 V versus Li/Li^+ (103 F g^{-1}) (**Figure 1**a,b). The symmetric and linear charge–discharge profile of YP-0 indicates pure double layer charging (Figure 1b). After the addition of 10 wt% of pyrene molecules (this weight fraction will be justified further down) into the composition of YP-0 electrodes (referred to as YP-10 in Table 1), a large Faradaic contribution corresponding to the pyrene oxidation[27,28,30,32] is depicted above 4 V during the first charge. This reaction enhances the capacity from 45 mAh $g^{-1}_{electrode}$ (YP-0) up to 75 mAh $g^{-1}_{electrode}$ (Figure 1a). It can be pointed out that the capacity on the first charge increases steadily with the initial amount of pyrene in the composite electrodes from 45 mAh g^{-1} (YP-0) to 90 mAh g^{-1} (YP-15) (Figure S2, Supporting Information). This extra capacity stems

Table 1. Justification of these compositions will be detailed in the text further below.

Acronyms	Components	Nominal compositions [wt%]	Electrode
YP-0	YP80-F, PVdF	95.2:4.8	Positive
YP-10	YP80, pyrene, and PVdF	85.7:9.5:4.8	Positive
YP-10-Li	YP80, pyrene, Li_3PO_4, and PVdF	79.4:9.3:6.6:4.7	Positive
Csp	Carbon SuperP and PVdF	90 : 10	Negative

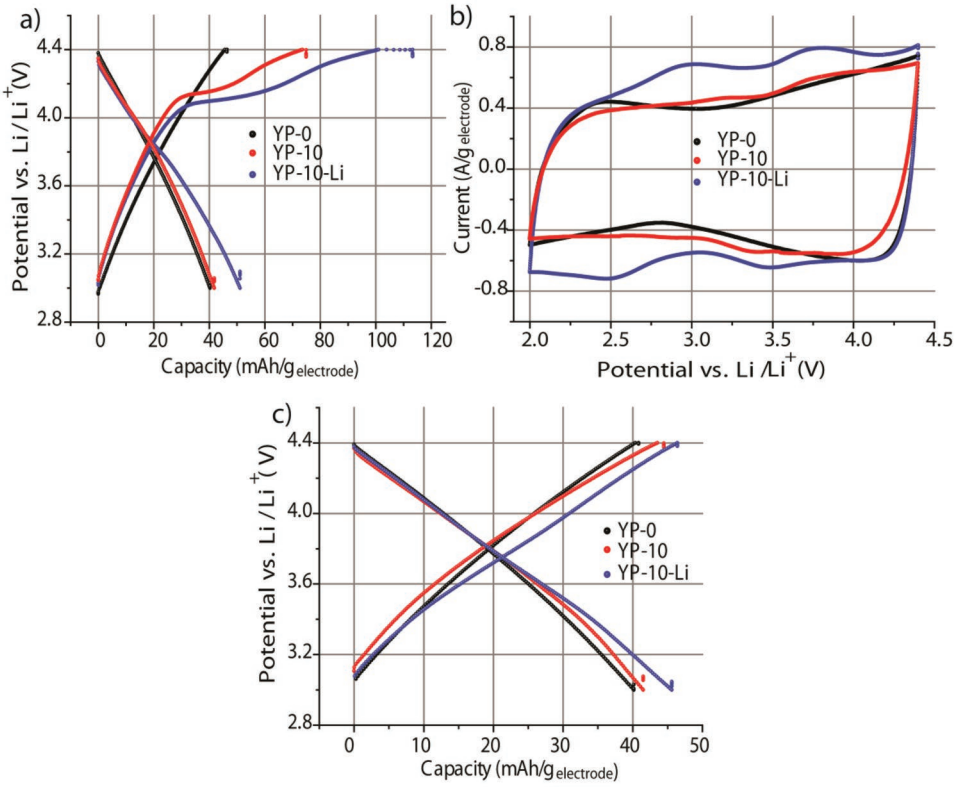

Figure 1. a) First charge–discharge profiles at a current density of 0.1 A $g^{-1}_{electrode}$, b) cyclic voltammetry at a scan rate of 5 mV s^{-1} after 20 cycles of charge-discharge. c) Charge-discharge profile of the fifth cycle. All measurements were carried out in Li metal half-cells with an excess of Li to avoid kinetic limitation from the negative electrode.

from both i) the electrons released during the irreversible electropolymerization of monomers and ii) consecutive oxidation of freshly formed oligomers/polymers according to the well known reversible p-doping process. The above two processes that occur during the first oxidation can be rationalized by the following reactions:[33]

$$n\mathrm{P}y \rightarrow (-\mathrm{P}y-)_n^{x+} nx\,\mathbf{PF_6^-} + ny\mathbf{H^+} + n(x+y)\,\mathbf{e^-} \quad (1)$$

where Py is the monomer, n is the number of monomers, y is the number of protons released per pyrene monomer, x and y are the number of reversible and irreversible electrons per pyrene molecule, respectively, while PF_6^- is the counter anion inserted in the p-doped polymer to balance the charge. As the pyrene electropolymerization is irreversible and occurs at potential lower than the electrolyte decomposition potential (<4.5 V vs Li^+/Li), this reaction is well suited to provide electrons for prelithiation without altering the cycle life of LIC. In subsequent cycles, the resulting pyrene oligomers undergo reversible p-doping according to the following reaction:

$$(-\mathrm{P}y-)_n^{x+} nx\,\mathbf{PF_6^-} + nx\mathbf{e^-} \leftrightarrow (-\mathrm{P}y-)_n + nx\,\mathbf{PF_6^-} \quad (2)$$

which enhances the capacity of the AC-based positive electrode (Figure S2c, Supporting Information).

The second key additive integrated into the positive electrode is a non-soluble inorganic base, Li_3PO_4. The latter plays a crucial role by scavenging protons (generated by Reaction 1) and by releasing a stoichiometric amount of Li^+ ions. Xu et al.[34] reported a Li base (lithium 2-trifluoromethyl-4,5-dicyanoimidazol) for scavenging HF produced in LIB at high temperature. Li_3PO_4 has several advantages: it is already mass produced at low cost, has a high volumetric density (2.4 g cm^{-3}), and is stable in ambient air, which is a key feature since no dry room is required during the manufacturing process. Furthermore, Li_3PO_4 is a well- known candidate for solid state electrolyte thanks to its high ionic conductivity (4.6×10^{-6} S cm^{-1} at 25 °C[35]), electrochemical stability[35–37] (Figure S3, Supporting Information). Its HF scavenging properties have been described in[31,38,39] and its pKa_3 (12.3) is expected to be low enough to avoid proton abstraction from carbonate solvents of the LP30 electrolyte. For the above reasons, Li_3PO_4 in principle is an ideal candidate to scavenge the protons released during the electropolymerization process through the following three reaction steps (we assume that H^+ are presumably solvated by carbonate electrolyte solvents and that the pKa values which apply to aqueous media are close to those found in organic media such as DMF:[40]

$$Li_3PO_4 + H^+ \rightarrow Li_2HPO_4 + Li^+ \quad \mathrm{p}Ka_3 - 12.3 \quad (3a)$$

$$Li_2HPO_4 + H^+ \rightarrow LiH_2PO_4 + Li^+ \quad \mathrm{p}Ka_2 - 7.2 \quad (3b)$$

$$LiH_2PO_4 + H^+ \rightarrow H_3PO_4 + Li^+ \quad \mathrm{p}Ka_1 - 2.1 \quad (3c)$$

To demonstrate the effectiveness of Li_3PO_4, we evaluated a composite electrode referred to as YP-10-Li that contains both the pyrene and the Li_3PO_4 additives according to the weight fraction defined in Table 1. SEM and electrode-dispersive X-ray (EDX) images of the YP-10-Li composite electrode are given in Figure S4 (Supporting Information). The EDX image indicates that ≈2–4 µm sized Li_3PO_4 particles are homogeneously dispersed within the electrode. The first charge–discharge profile of YP-10-Li at 0.1 A $g^{-1}_{electrode}$ in a Li metal half-cell is compared with those of YP-80 and YP-10 in Figure 1a. Remarkably, even though YP-10 and YP-10-Li contain nearly the same amount of pyrene(10%), the capacity upon first oxidation is enhanced by 46 %, i.e., from 75 (YP-10) to 110 mAh g^{-1} (YP-10-Li). Notably, this effect stems from proton scavenging property of Li_3PO_4 that favor reactions 3a and 3c. Indeed, the use of a base was shown to favor the electropolymerization process and yields longer polymer chains.[41–43] Upon 20 cycles, both CV profiles (Figure 1b) and charge–discharge curves (Figure 1c) of YP-10-Li display a strong Faradaic contribution supporting that more redox active/p-doped polymer is produced after loading Li_3PO_4.[33] This enables to increase the capacity during discharge by 16%, when considering the mass of both AC and pyrene and, by 7 % for the whole electrode mass (45 mAh $g^{-1}_{electrode}$ for YP-10-Li and 42 mAh $g^{-1}_{electrode}$ for YP-10, Figure 1c). Taking into account both, the irreversible and reversible capacities of YP-0, YP-10, and YP-10-Li, the capacity contribution of the pyrene component during the first oxidation (=prelithiation capacity) is found to be 698 mAh g^{-1}_{pyrene} for YP-10-Li and 368 mAh g^{-1}_{pyrene} for YP-10, while the reversible specific capacity during the subsequent reduction step is 169 mAh g^{-1}_{pyrene} for YP-10-Li and 30 mAh g^{-1}_{pyrene} for YP-10. Taking into the mass of both the pyrene and Li_3PO_4, this reversible specific capacity comes to nearly 100 mAh $g^{-1}_{(pyrene+Li3PO4)}$ for YP-10-Li and constitutes the best one so far for prelithiation additives. Accordingly, the electropolymerization process releases ≈2.5 and 4.0 protons by each pyrene molecule in YP-10 and YP-10-Li, respectively, which reiterates the double role Li_3PO_4 which also serves to boost the polymerization reactions. In addition, considering the molar ratio of ≈3.2 between the protons released upon electropolymerization and the Li_3PO_4 content selected in YP-10-Li (Table 1), Li_3PO_4 in principle should fully react according to the three acid-base reactions listed above.

To gain better insight into the ionic exchange efficiency (=proton scavenging capability) of Li_3PO_4, operando XRD was conducted during the first electrochemical cycle of YP-10-Li. The reference XRD diagrams of ball-milled β-Li_3PO_4 and the separator used in the operando cell are compared to that obtained for YP-10-Li in its initial state in **Figure 2**a. Despite a rather low weight fraction of Li_3PO_4 in the electrode (6.6 wt%), the intensities of the (210), (011), (111), (020), and (220) lines are high enough to determine the amount of Li_3PO_4. The latter is constant until the potential of the YP-10-Li electrode reaches that of pyrene electropolymerization (4.0 V vs Li/Li^+) and vanishes at 4.2 V (Figure 2b,c). Li_2HPO_4 or LiH_2PO_4, that are insoluble in LP30 electrolyte, were not detected by XRD. The reaction of Li_3PO_4 is confirmed by ex situ Raman spectroscopy as shown by the shift of the symmetrical stretching vibration ($\nu_1PO_4^-$)[44] from 943 cm^{-1} (before oxidation) to 1048 cm^{-1} (upon oxidation to 4.4 V) (Figure S5, Supporting Information). We note, however, there is an ambiguity in assigning this peak to either H_3PO_4 or LiH_2PO_4 due to their overlapping in this region.[45]

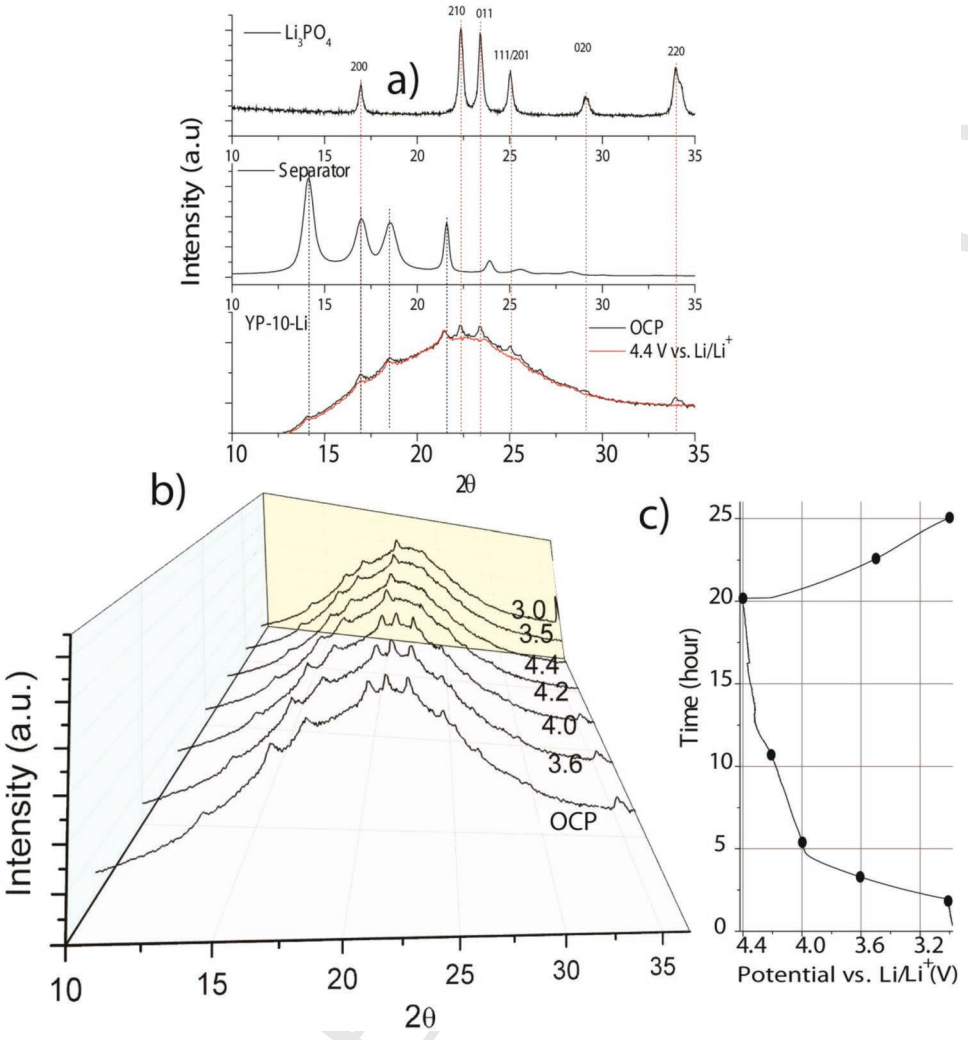

Figure 2. a) Comparative XRD diagrams of Li_3PO_4, separator, and YP-10-Li in the operando cell at OCP and at 4.4 V versus Li/Li^+. b) Operando XRD diagrams of YP-10-Li at various potentials measured during charge–discharge carried at 7.5 mA g^{-1} and corresponding electrochemical responses in (c).

To clarify the role of Li_3PO_4, the organic carbonate solvent[46] based electrolytes were recovered from the Li half-cells of YP-10 and YP-10-Li after 33 cycles and were evaluated by ^1H, ^{31}P, and ^{19}F NMR measurements. In the case of YP-10, ^{31}P NMR (**Figure 3**a) reveals a triplet peak centered at −20.7 ppm in addition to the signal associated with PF_6^-[47] at −146.1 ppm. This new signal that matches the doublet centered at 84.5 ppm in the ^{19}F NMR spectra (Figure 3b) is attributed to R-OPF_2 (R=OH or CH_3) species.[47,48] This type of compounds would result from the hydrolysis of PF_6^- anions by the reaction with protons. Importantly, R-OPF_2 is not detected for YP-10-Li, which reiterates the efficiency of Li_3PO_4 in exchanging released H^+. Therefore the combination of operando XRD, Raman spectroscopy as well as ^{31}P, and ^{19}F NMR confirm the proton scavenging properties of Li_3PO_4 during electropolymerization of pyrene. We note, however, that no soluble H_3PO_4 was detected by ^{31}P NMR measurements although the theoretical ratio H^+/Li_3PO_4 should be ≈3.2. Several explanations can be proposed: a) H_3PO_4 is not formed because part of the protons react with the Li metal electrode leaving (insoluble) amorphous LiH_2PO_4 and Li_2HPO_4 in the YP-10-Li electrode, b) acidic H_3PO_4 diffuses to Li counter/reference electrodes, where it precipitates upon acid-base H^+/Li^+ exchange and, c) H_3PO_4 is trapped at the surface of YP-80. More insight will be gained from full cell investigations in the next section. Noteworthy, aromatic ^1H signals that would represent dissolved pyrene monomers or oligomers were not observed (Figure S6, Supporting Information), which confirms the stability of the YP-80/ polymer assembly on cycling. In addition, pyrene and Li_3PO_4 additives do not affect the power capability (Figure S7a, Supporting Information), long-term stability (Figure S7b, Supporting Information), and self-discharge properties (Figure S8, Supporting Information) of the YP80 material upon in situ reactions, therefore, confirming the robustness and efficiency of the present concept.

In brief, the combined utilization of a p-type electron source with a nonsoluble base, Li_3PO_4, allows in situ generation of electrons and lithium ions. Overall the combination of these additives provides a prelithiation capacity of 408 mAh $g^{-1}_{(Li3PO4+Pyrene)}$. On subsequent cycles, the freshly electropolymerized pyrene conducting polymer enhances the

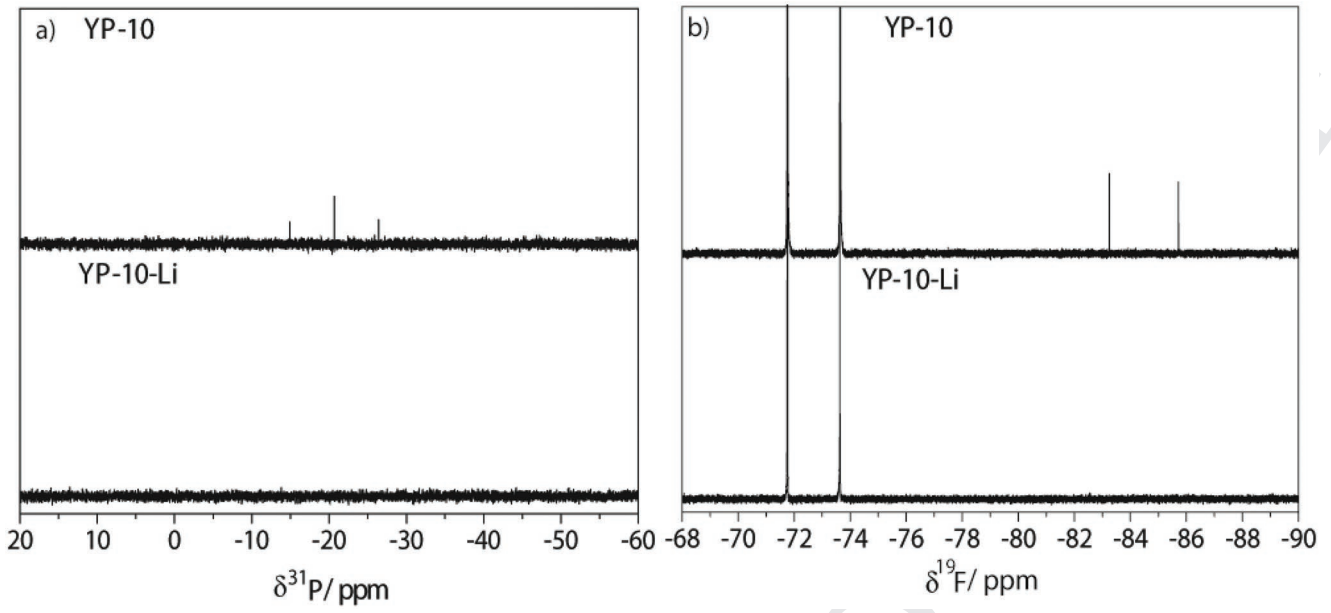

Figure 3. NMR spectra of cycled electrolyte from Li metal cell: a) ^{31}P and b) ^{19}F.

capacity of the positive electrode through the anionic assisted p-doping process.

To validate the cascade-type prelithiation approach in a fullcell, we used a cheap carbon black powder as the negative electrode (Super-P, Csp) with a specific surface area (SSA) of 63 $m^2\ g^{-1}$, a tap density of 0.1 g cm^{-3}, and a particle size of ≈35–40 nm. Csp was selected as a model negative electrode for two main reasons: as reported in our previous work[19] i) the irreversible capacity of 166 % during the first cycle is similar to that of the new generation of anodes in LIC (**Figure 4**)[10] and ii) it shows an excellent cyclability and power capability.[19]

The potential of each electrode was monitored using a Li metal reference electrode. The mass ratio (R) of the positive to the negative electrode was determined by taking into consideration the capacity during the first charge of Csp (400 mAh g^{-1}), YP (45 mAh g^{-1}), YP-10 (75 mAh g^{-1}) and YP-10-Li (100 mAh g^{-1}), i.e., R = 9.3, 6.1, and 4.1 for YP, YP-10, and YP-10-Li, respectively. Potential versus capacity profiles are plotted for each electrode (**Figure 5**a), where the capacity is normalized to the mass of respective electrodes. In case of a YP-0 full cell, the Csp electrode nearly behaves like in a Li metal half-cell (Figure 5a) and delivers a capacity of 437 mAh g^{-1} upon the first charge. However, in case of YP-10, this capacity is much higher (820 mAh g^{-1}, Figure 5a). Given that the electrochemical profile of YP-10 is very similar to that observed in a Li metal half-cell up to 4.0 V versus Li/Li^+, this extracapacity arises from the electropolymerization process above 4.0 V versus Li/Li^+, which should release 1.84×10^{-3} M $g^{-1}_{\text{positive electode}}$ of H^+ accordingly. Assuming all these protons are reduced to H_2 during the first cycle, they would generate a capacity of 300 mAh $g^{-1}_{\text{negative electode}}$. Thus, it is reasonable to assume that the plateau detected at 0.6 V for YP-10 corresponds to H_2 production in addition to SEI formation and Li insertion in Csp[13] (Figure 5a). Moreover, H_2 is known to take part in redox shuttle mechanism (H^+/H_2) in the cell.[49] This can further enhance the irreversible capacity to up to 130 mAh g^{-1} instead of 75 mAh g^{-1}, as observed in a Li metal half-cell where H^+ is presumably trapped at the Li surface (Figure S9b, Supporting Information). On the contrary, for YP-10-Li, the potential profile of the Csp electrode is very similar to that of YP-0, which reiterates the remarkable proton scavenging property of Li_3PO_4. As a consequence, the positive and negative electrodes deliver very similar capacity (Figure 5a) in Li metal half-cells (Figure S9a, Supporting Information).

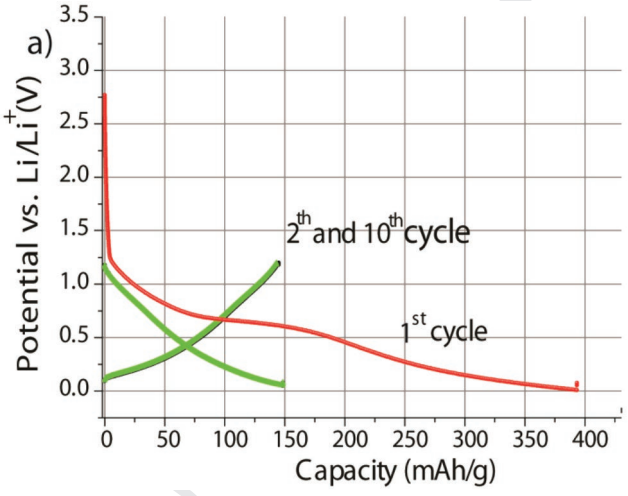

Figure 4. a) First charge–discharge profiles of Csp at a current density of 0.1 A $g^{-1}_{\text{positive electrode}}$. Measurements were carried out in Li metal half-cells.

Long-term cycling stability measurements of YP, YP-10, and YP-10-Li were carried out in two-electrode Swagelok cells. Presumably due to H_2 evolution and due to the H^+/H_2 internal couple, the YP-10 cell failed within 100 cycles (**Figure 6**a). Concomitantly, the Coulombic efficiency, which is less than 75%

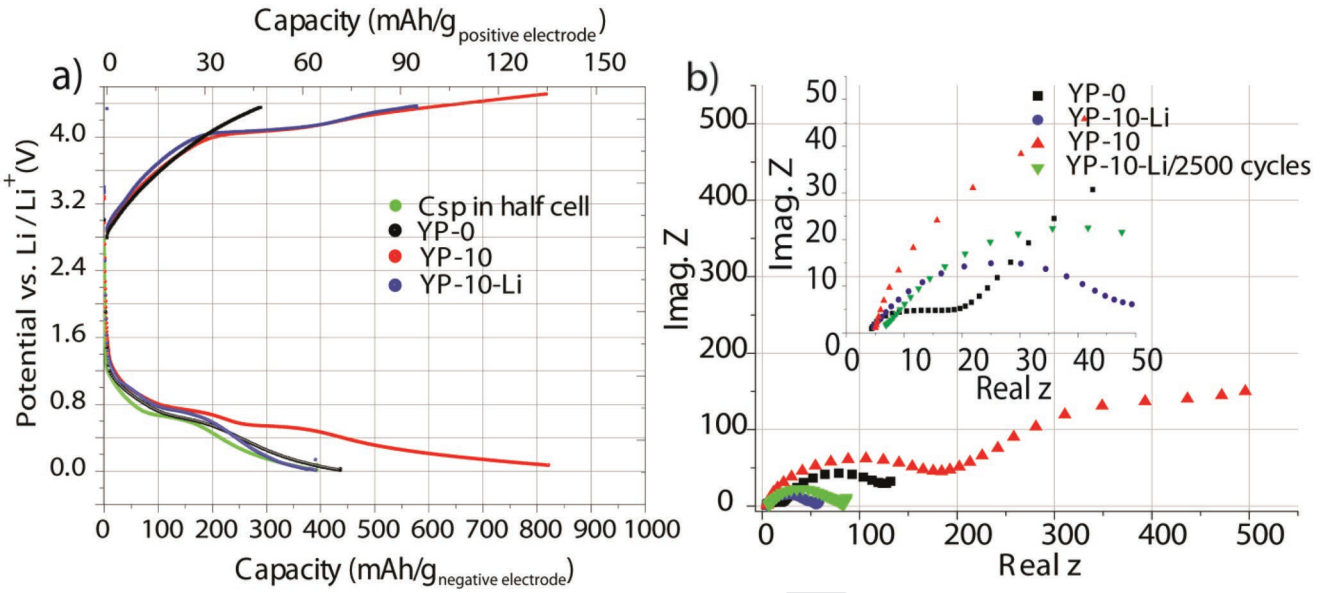

Figure 5. a) Potential versus capacity profile of positive electrode (YP, YP-10, and YP-10-Li) and negative electrode (Csp) electrode in three-electrode full cell using a Li metal reference electrode. b) Nyquist plot from EIS measurements of full-cells in fully charged state after 100 cycles.

for YP-10 (Figure 6a), mirrors major side reactions. The EIS spectrum collected after 100 cycles (Figure 6b) evidences a significant increase in charge-transfer resistance, which is accompanied by the occurrence of two new semicircles, one in the highest frequency region and another in the lowest frequency region (Figure 6b).

Remarkably, the cycling stability of the YP-0 cell is not as good as that of YP-10-Li cell or that obtained in our previous study[13] where YP-0 was prelithiated using a Li electrode. Moreover, YP-10-Li shows two charge-transfer resistances (R_{ct} = 44 + 8.25 Ohms) that are lower than those of YP-0 (11.28 + 103.6 ohms) and YP-10 (161 + 264 ohms), presumably due to the decreased impedance of the prelithiated Csp electrode.[50] We note that in our conditions, Li ions depletion occurring in the electrolyte of YP-0 and YP-10 (≈4% and 8%) are too low to be detected by EIS (Figure 6c). Nevertheless, as observed by others,[51,52] these results reconfirm the positive impact of prelithiation on both cycle life and impedance of full cells.

The capacity of the YP-10-Li full cell reaches 17 mAh $g^{-1}_{electrodes}$ (50th cycle, 0.1 A $g^{-1}_{electrode}$) by considering the total mass of the two Csp and YP-10-Li electrodes (Figure 6b). Whereas, YP-0 and YP-10 full cell only show 6.3 and 9.2 mAh $g^{-1}_{electrodes}$ respectively (Figure 6b). This overwhelming capacity incurred by YP-10-Li stems from the present prelithiation strategy that allows simultaneously to decrease the weight ratio of the positive electrode by 200% and to increase its capacity by 13%. Overall an energy density of 63 Wh $Kg^{-1}_{electrodes}$ is obtained for YP-10-Li. This value compares well with 30 Wh $Kg^{-1}_{electrodes}$ commonly measured for standard electrochemical capacitors, with a capacitance of 25 F $g^{-1}_{electrodes}$ and a 3 V cell voltage. We note that most of the reports do not take into account the prelithiation step to derive energy density values (further details are provided in Table S1, Supporting Information). The robustness of the YP-10-Li full cell is proven by its remarkable capacity retention over 2200 cycles (Figure 6c) and a minor increase of R_{ct} (Figure 5b). Moreover, the stable and high Coulombic efficiency demonstrates the absence of the degradation of the SEI and, as shown by NMR results in Figure 3, supports pyrene-based species do not dissolve in the electrolyte. Furthermore, it is clear that the efficiency of this cascade-type prelithiation mechanism can be improved further in future because the specific and volumetric capacities associated with pyrene-electropolymerization and p-doping has been shown to be much higher depending on the pyrene derivatives.[27–29] In addition is well established in the literature[27–29] that the mass fraction of redox active pyrene derivative can be increased significantly depending on the type of carbon additives used in the positive electrode. In conclusion, the average graphitization state of the carbon material at the positive electrode is a vital leverage factor.[27,28] Lastly, the number of exchangeable Li^+ ions per mass and volume of the base is a crucial aspect that should also clearly be optimized.

3. Conclusion

A cascade-type mechanism is proposed for the first time to prelithiate the negative carbon electrode of an LIC. This approach is based on two consecutive irreversible reactions occurring within the positive electrode during the first charge: i) oxidative electropolymerization of pyrene moieties produces protons; ii) these protons are captured by an insoluble and highly ionic conducting base, Li_3PO_4, which not only triggers a stoichiometric release of Li ions into the electrolyte but also enhances the electropolymerization reaction. (^1H, ^{19}F, and ^{31}P) NMR spectroscopy as well as operando XRD and Raman spectroscopy support this mechanism, which delivers 136 mAh g^{-1}_{Li3PO4} for each H^+/Li^+ exchange. Substantial advantages were shown to incur by decoupling the source of lithium and electrons since the physicochemical properties of the two additives can be independently tailored to effectively avoid

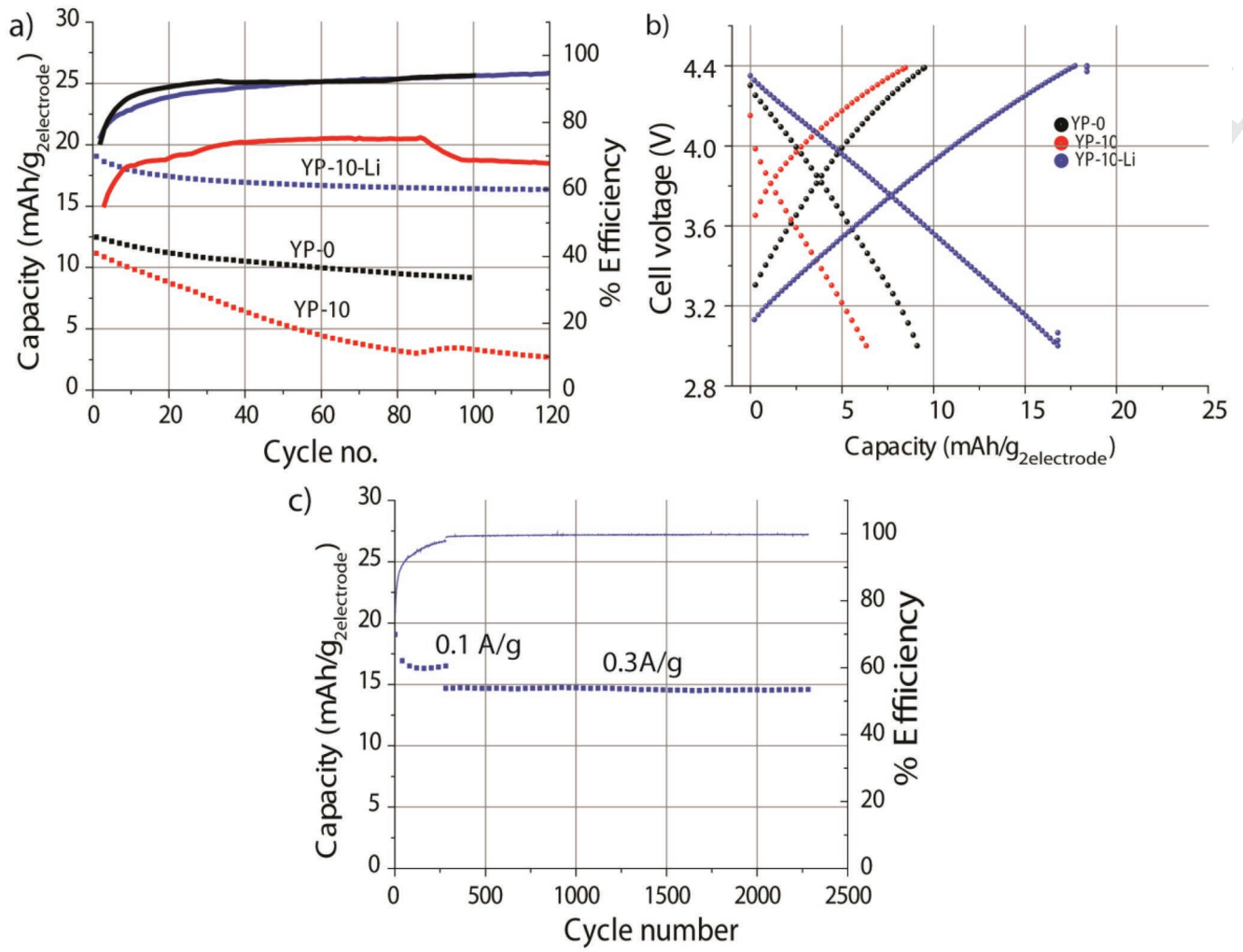

Figure 6. a) Capacity retention and Coulombic efficiency of YP-0, YP-10 and YP-10-Li full cells at a current density of 0.1 A $g^{-1}_{positive\ electrode}$. b) 50th charge–discharge profile of full-cell at a current density of 0.1 A g^{-1}. c) Long-term cycling performance of YP-10-Li.

reactivity with ambient air and solvent during electrode processing while enhancing the reversible specific capacity of the positive electrode through p-doping. In summary, the effectiveness and versatility offered by this cascade-type approach may well provide a great leap forward into low-cost and industry-relevant path to deal with a major scientific bottleneck revolving around the issue of prelithiation.

4. Experimental Section

Materials: Pyrene and Li_3PO_4 were purchased from Aldrich Chemicals, LP-30 (1 M $LiPF_6$ in 50:50 wt% ethylene carbonate: dimethyl carbonate) from BASF, Super P(Csp) conductive carbon black was purchased from TIMCAL, activated carbon (YP-80F) was purchased from Kuraraychemical, PVdF binder from Kynar and, *N*-methylpyrrolidone (NMP) from Aldrich. Li_3PO_4 was ball milled for 3 h at a speed of 700 rpm using a Pulverisette 7 premium line from Fritsch-international and dried at 250 °C overnight to remove residual moisture. All other chemicals were used as received.

Electrode Preparation: All electrode inks were prepared by ball milling electrode materials in NMP for 30 min at 600 rpm. Inks were then coated on a current collector by roll coating. Aluminum foil was used for the positive electrode, and the copper foil was used for the negative electrode. Mass loadings were 4–5 mg cm^{-2} for positive electrodes and 1–2 mg cm^{-2} for the negative one. Electropolymerization of pyrene moieties was carried out by galvanostatic cycling at 0.1 A g^{-1} within a 2–4.4 V versus Li^+/Li potential window. Nominal compositions of all samples used onwards along with their acronyms are gathered in in Table 1. Justification of these compositions will be detailed in the text further below.

Electrochemical Characterization: Modified Swagelok cells with an electrode diameter of 12 mm were used for electrochemical measurement. Electrodes were initially dried at 80 °C overnight, followed by 90 °C overnight under vacuum and then cut into the specific dimension. Cell assembly was carried out in a moister free glove box (H_2O < 1 ppm, O_2 < 0.3 ppm) using Whatman glass fiber separator soaked in the LP30 electrolyte. All electrochemical measurements were monitored using Bio-Logic VMP-2 or -3 potentiostat. Reference and counter electrodes were Li metal until specified separately. Cyclic voltammetry was carried out at a scan rate of 5 mV s^{-1}, and charge–discharge was at a current density range of 0.5–10 mA cm^{-2}. All the potentials were reported against Li^+/Li reference in half cells. Electrochemical impedance spectroscopy (EIS) was performed from 200 kHz to 0.1 Hz with a sinusoidal amplitude of 10 mV (V_{rms} = 7.07 mV).

For the full cell, carbon black (Csp) was used as the negative electrode and either YP-0, YP-10, or YP-10-Li as the positive electrode in a voltage range of 3 to 4.4 V. Considering the capacity of Csp on the first charge, a mass ratio of positive to negative electrode of 9.3, 6.1, and 4.1 was used for YP-0, YP-10, or YP-10-Li, respectively. Initial cycling was carried at a current density of 0.1 A g^{-1} and followed by long-term cycling at 0.3 A g^{-1}. The power characteristics were evaluated using current densities from 0.1 to 3 A g^{-1}. Energy density and power density was calculated using Ec-Lab software with $E = V*I*t$ (I is the current, V is the average-voltage of the full cell ≈3.7 V and t is discharge time) and $P = E/t$, respectively.

Other Characterizations: Scanning electron microscopy (SEM) was carried out in Jeol JSM-7600F. Raman spectroscopy was carried out using SENTERRA (Bruker) using 532 nm laser beam. In Operando XRD was conducted with a Bruker D8 Advance diffractometer using a home-made airtight cell in which the YP-10-Li electrode was cast over a beryllium current collector and separated from Li counter and reference electrodes by a monolayer polypropylene separator (Celgard 2500). The cell assembly was carried out in a dry room, and LP-30 was used as the electrolyte. The electrode was continuously scanned in Bragg Brentano geometry between $2\theta = 10°$ to 40° during the charge and discharge at 0.01 A g^{-1}; one scan lasts for 15 min.

NMR spectra were recorded on an advance II HD spectrometer (Bruker, USA) at 400 MHz (^{1}H). SiMe4 (^{1}H), CCl3F (^{19}F), and H_3PO_4 (^{31}P) were used as primary standards. Upon cycling from 0.05 to 50 A g^{-1} for 33 cycles, electrodes and separators were removed from coin cells and washed by immersion in 500 µL of deuterated acetonitrile. The resulting solution was filtered using a PTFE membrane and analyzed.

Supporting Information

Supporting Information is available from the Wiley Online Library or from the author.

Conflict of Interest

The authors declare no conflict of interest.

Keywords

electropolymerization, lithium base, lithium ion battery, lithium-ion capacitor, operando XRD, prelithiation, proton–lithium exchange

Received: January 8, 2019
Revised: February 18, 2019
Published online:

[1] D. O. Akinyele, R. K. Rayudu, *Sustainable Energy Technol. Assess.* **2014**, *8*, 74.
[2] M. Aneke, M. Wang, *Appl. Energy* **2016**, *179*, 350.
[3] R. Schmuch, R. Wagner, G. Hörpel, T. Placke, M. Winter, *Nat. Energy* **2018**, *3*, 267.
[4] M. Winter, R. J. Brodd, *Chem. Rev.* **2004**, *104*, 4245.
[5] A. Burke, *Electrochim. Acta* **2007**, *53*, 1083.
[6] G. E. Blomgren, *J. Electrochem. Soc.* **2017**, *164*, A5019.
[7] T. Placke, R. Kloepsch, S. Dühnen, M. Winter, *J. Solid State Electrochem.* **2017**, *21*, 1939.
[8] J. Ding, W. Hu, E. Paek, D. Mitlin, *Chem. Rev.* **2018**, *118*, 6457.
[9] P. Meister, H. Jia, J. Li, R. Kloepsch, M. Winter, T. Placke, *Chem. Mater.* **2016**, *28*, 7203.
[10] F. Holtstiege, P. Bärmann, R. Nölle, M. Winter, T. Placke, *Batteries* **2018**, *4*, 4.
[11] N. Dupré, P. Moreau, E. De Vito, L. Quazuguel, M. Boniface, H. Kren, P. Bayle-Guillemaud, D. Guyomard, *Chem. Mater.* **2017**, *29*, 8132.
[12] M. Winter, *Z. Phys. Chem.* **2009**, *223*, 1395.
[13] M. Kim, F. Xu, J. H. Lee, C. Jung, S. M. Hong, Q. M. Zhang, C. M. Koo, *J. Mater. Chem. A* **2014**, *2*, 10029.
[14] S. Tasaki, N. Ando, M. Nagai, A. Shirakami, K. Matsui, Y. Hato, US7733629 B2, **2014**.
[15] S. Tasaki, M. Nagai, N. Ando, US20090246626 A1, **2006**.
[16] M. Mizukami, K. Nansaka, N. Ando, EP2541567 A1, **2010**.
[17] D. Aurbach, E. Zinigrad, Y. Cohen, H. Teller, *Solid State Ionics* **2002**, *148*, 405.
[18] F. Holtstiege, R. Schmuch, M. Winter, G. Brunklaus, T. Placke, *J. Power Sources* **2018**, *378*, 522.
[19] B. Anothumakkool, N. Dupré, P. Moreau, D. Guyomard, T. Brousse, J. Gaubicher, *J. Power Sources* **2018**, *378*, 628.
[20] J. Li, J. Guo, P. Li, L. Wang, Y. Huang, *Int. J. Electrochem. Sci.* **2017**, *12*, 3212.
[21] N. Xu, X. Sun, F. Zhao, X. Jin, X. Zhang, K. Wang, K. Huang, Y. Ma, *Electrochim. Acta* **2017**, *236*, 443.
[22] W. J. Cao, J. P. Zheng, *J. Power Sources* **2012**, *213*, 180.
[23] K. Park, B.-C. C. Yu, J. B. Goodenough, *Adv. Energy Mater.* **2016**, *6*, 1502534.
[24] V. Aravindan, N. Arun, N. Shubha, J. Sundaramurthy, S. Madhavi, *Electrochim. Acta* **2016**, *215*, 647.
[25] P. Jeżowski, O. Crosnier, E. Deunf, P. Poizot, F. Béguin, T. Brousse, *Nat. Mater.* **2017**, *17*, 167.
[26] D. Shanmukaraj, S. Grugeon, S. Laruelle, G. Douglade, J.-M. Tarascon, M. Armand, *Electrochem. Commun.* **2010**, *12*, 1344.
[27] B. Anothumakkool, P.-L. Taberna, B. Daffos, P. Simon, Y. Ahmad-Baraza, C. Ewels, T. Brousse, J. Gaubicher, J. Gaubicher, *J. Mater. Chem. A* **2017**, *5*, 1488.
[28] L. Madec, A. Bouvrée, P. Blanchard, C. Cougnon, T. Brousse, B. Lestriez, D. Guyomard, J. Gaubicher, *Energy Environ. Sci.* **2012**, *5*, 5379.
[29] J. C. Bachman, R. Kavian, D. J. Graham, D. Y. Kim, S. Noda, D. G. Nocera, Y. Shao-Horn, S. W. Lee, *Nat. Commun.* **2015**, *6*, 7040.
[30] R. J. Waltman, J. Bargon, *Can. J. Chem.* **1986**, *64*, 76.
[31] C. H. Jo, D. H. Cho, H. J. Noh, H. Yashiro, Y. K. Sun, S. T. Myung, *Nano Res.* **2015**, *8*, 1464.
[32] R. J. Waltman, A. F. Diaz, J. Bargon, *J. Phys. Chem.* **1984**, *88*, 4343.
[33] J. Heinze, B. A. Frontana-Uribe, S. Ludwigs, *Chem. Rev.* **2010**, *110*, 4724.
[34] C. Xu, S. Renault, M. Ebadi, Z. Wang, E. Björklund, D. Guyomard, D. Brandell, K. Edström, T. Gustafsson, *Chem. Mater.* **2017**, *29*, 2254.
[35] N. Kuwata, N. Iwagami, J. Kawamura, *Solid State Ionics* **2009**, *180*, 644.
[36] N. Kuwata, N. Iwagami, Y. Matsuda, Y. Tanji, J. Kawamura, *ECS Trans.* **2009**, *16*, 53–60.
[37] N. Kuwata, N. Iwagami, Y. Tanji, Y. Matsuda, J. Kawamura, *J. Electrochem. Soc.* **2010**, *157*, A521.
[38] C.-F. F. Sun, J. Hu, P. Wang, X.-Y. Y. Cheng, S. B. Lee, Y. Wang, B. Lee, Y. Wang, *Nano Lett.* **2016**, *16*, 5875.
[39] H. Liu, C. Chen, C. Du, X. He, G. Yin, B. Song, P. Zuo, X. Cheng, Y. Ma, Y. Gao, *J. Mater. Chem. A* **2015**, *3*, 2634.
[40] L. P. Safonova, Y. A. Fadeeva, A. A. Pryakhin, *Russ. J. Phys. Chem. A* **2009**, *83*, 1747.
[41] M. Zhou, J. Heinze, *J. Phys. Chem. B* **1999**, *103*, 8451.
[42] G. Sabouraud, S. Sadki, N. Brodie, *Chem. Soc. Rev.* **2000**, *29*, 283.

[43] J. Heinze, H. John, M. Dietrich, P. Tschuncky, *Synth. Met.* **2001**, *119*, 49.
[44] L. Popović, B. Manoun, D. De Waal, M. K. Nieuwoudt, J. D. Comins, *J. Raman Spectrosc.* **2003**, *34*, 77.
[45] W. W. Rudolph, *Dalton Trans.* **2010**, *39*, 9642.
[46] R. W. Schmitz, P. Murmann, R. Schmitz, R. Müller, L. Krämer, J. Kasnatscheew, P. Isken, P. Niehoff, S. Nowak, G. V. Röschenthaler, N. Ignatiev, P. Sartori, S. Passerini, M. Kunze, A. Lex-Balducci, C. Schreiner, I. Cekic-Laskovic, M. Winter, *Prog. Solid State Chem.* **2014**, *42*, 65.
[47] S. Wiemers-Meyer, M. Winter, S. Nowak, *Phys. Chem. Chem. Phys.* **2016**, *18*, 26595.
[48] S. Nowak, M. Winter, *J. Electrochem. Soc.* **2015**, *162*, A2500.
[49] W. C. Barrette, D. T. Sawyer, *Anal. Chem.* **1984**, *56*, 653.
[50] M. Cai, X. Sun, Y. Nie, W. Chen, Z. Qiu, L. Chen, Z. Liu, H. Tang, *Nano* **2017**, *12*, 1750051.
[51] Y.-G. Lim, D. Kim, J.-M. Lim, J.-S. Kim, J.-S. Yu, Y.-J. Kim, D. Byun, M. Cho, K. Cho, M.-S. Park, *J. Mater. Chem. A* **2015**, *3*, 12377.
[52] S. Kumagai, T. Ishikawa, N. Sawa, *J. Energy Storage* **2015**, *2*, 1.

ADVANCED ENERGY MATERIALS

Reprint Order Form 2019
- please return with your proofs -

Editorial Office:

Wiley-VCH Verlag, Boschstrasse 12
69469 Weinheim, Germany

Tel.: (+49) 6201 606 531
Fax: (+49) 6201 606 500

E-mail: advenergymat@wiley-vch.de
http://www.advenergymat.de

Manuscript No. _____

Please send me and bill me for

☐ no. of **reprints** via ☐ airmail (+ 25 Euro) ☐ surface mail

☐ **high-resolution PDF file** (330 Euro).

My e-mail address:

_____

Please note: It is not permitted to present the PDF file on the internet or on company homepages

★**Special Offer**★ If you order 200 or more reprints you will get a PDF file for half price.

Information regarding VAT
Please note that from German sales tax point of view, the charge for **Reprints, Issues or Posters** is considered as **"supply of goods"** and therefore, in general, such delivery is a subject to German sales tax. However,this regulation has no impact on customers located outside of the European Union. Deliveries to customers outside the Community are automatically tax-exempt. Deliveries within the Community to institutional customers outside of Germany are exempted from the German tax (VAT) only if the customer provides the supplier with his/her VAT number. The VAT number (value added tax identification number) is a tax registration number used in the countries of the European Union to identify corporate entities doing business there. It starts with a country code (e.g. FR for France, GB for Great Britain) and follows by numbers.

Cover Posters

Posters are available of all the published covers and frontispieces in two sizes

☐ DIN A2 42 x 60 cm/ 17 x 24in (one copy: **39 Euro**)

☐ DIN A1 60 x 84 cm/ 24 x 33in (one copy: **49 Euro**)

Postage for shipping posters overseas by airmail:
+ 25 Euro

Postage for shipping posters within Europe by surface mail:
+ 15 Euro

Mail reprints / cover posters to:

_____
_____
_____
_____
_____

Invoice address:

_____
_____
_____
_____
_____

Date, Signature **Stamp**

VAT no.: _____
(institutes / companies in EU countries only)

Purchase Order No.: _____

Credit Card Payment

VISA, MasterCard, AMERICAN EXPRESS
Please use the Credit Card Token Generator located at the website below to create a token for secure payment. The token will be used instead of your credit card number.

Credit Card Token Generator:
https://www.wiley-vch.de/editorial_production/index.php

Please transfer your token number to the space below.

Credit Card Token Number:

Price list for reprints (The prices include mailing and handling charges. All Wiley-VCH prices are exclusive of VAT)

No. of pages	Price (in Euro) for orders of 50 copies	100 copies	150 copies	200 copies	300 copies	500 copies
1-4	345	395	425	445	548	752
5-8	490	573	608	636	784	1077
9-12	640	739	786	824	1016	1396
13-16	780	900	958	1004	1237	1701
17-20	930	1070	1138	1196	1489	2022
for every additional 4 pages	147	169	175	188	231	315

★ **Special Offer** ★ If you order 200 or more reprints you will get a PDF file for half price.

Wiley-VCH Verlag GmbH & Co. KGaA; Location of the Company: Weinheim;
Chairman of the Supervisory Board: John Kritzmacher,
Trade Register: Mannheim, HRB 432833, General Partner: John Wiley & Sons GmbH,
Location: Weinheim, Trade Register Mannheim, HRB 432296,
Managing Directors: Sabine Steinbach, Dr. Guido F. Herrmann

WILEY-VCH